M-1

PERFORMANCE OF A Ka-BAND SATELLITE SYSTEM UNDER VARIABLE TRANSMITTED SIGNAL POWER CONDITIONS

Gene Fujikawa and Robert Kerczewski

National Aeronautics and Space Administration
Lewis Research Center
Cleveland, Ohio 44135

Abstract

A laboratory hardware-based satellite communication system simulator has been used to measure the effects of transmitted signal power changes on the performance of a Ka-band system. Such power changes can be used to compensate for signal fade due to rain attenuation. This paper presents and discusses the results of these measurements.

Introduction

Among the problems associated with Ka-band satellite communications systems are the effects of signal fading, primarily due to rain attenuation. One possible solution to this problem is to offset the fading by temporarily increasing the transmitted signal power. The effects of these power level changes on the transmission quality of the system must be understood in order to implement such a system.

With this in mind, a series of tests was conducted at NASA's Lewis Research Center to determine the effects of varying the transmitted power level on the system performance. Using a hardware-based system simulating an end-to-end satellite communications link, transmission tests were performed while varying the satellite downlink output power between three different power levels. To implement these power level changes, an experimental 17.7 to 20.2 GHz multi-power-mode traveling wave tube amplifier (TWTA) was used as the satellite downlink high power amplifier. Tests were conducted using CW and digitally modulated signals, while varying the amplifier drive levels and other system parameters. The results of these tests are presented and discussed below.

Test System Description

The critical elements of a Ka-band TDMA satellite communications system have been developed under NASA-sponsored technology programs. These components, integrated with microwave and digital systems designed and built in-house, form a flexible satellite communications link simulator, shown in Fig. 1. A helix-type TWTA with anode voltage control gives the simulator its multi-power-mode capability. An associated power processor unit adjusts the anode voltage to one of three settings to allow operation in three distinct power modes. Operational data for the TWTA is given in Table I.

The output of the digital data transmission tests is a measurement of the system bit error rate (BER) as a function of received signal to noise ratio (Eb/No). Pseudorandom data at 220 Mbps was modulated using a serial minimum-shift-keyed (SMSK) format and transmitted through the system over a 330 MHz bandlimited channel. A calibrated amount of noise was introduced into the downlink signal path to achieve a range of values For Eb/No. The signal was demodulated and the received bits checked against a stored replica of the original data. A BER versus Eb/No comparison was then obtained.

Test Results

End-to-end system BER measurements were performed for each of the three power modes while varying the frequency and the TWTA operating point. Three frequency bands (Fig. 2), having different transmission characteristics, were used for testing. The TWTA operating point was varied between linear, 1 dB compression, and saturation. Amplitude and group delay response, AM/PM conversion, third order intermodulation, and system noise output were investigated for each of the system variations described above. An examination was made of the system BER performance variation due to the changes in power mode. The effects of the transmission distortions and TWTA operating points on digital data transmission were also examined.

The results of the BER measurements are summarized in Table II. The additional Eb/No required to maintain a BER of $5x10^{-7}$, as compared to the theoretical SMSK curve, is given for each of the system configurations mentioned above. The last column in the table, showing the maximum deviation of Eb/No between modes for a given operating point and frequency band, is of primary interest.

For two cases (Band B at saturation and at 1 dB compression), there was negligible deviation in the measured BER between modes. For the other cases the deviation ranges from 0.54 to 1.72 dB. This can be attributed to the variation between power modes of measured system distortions, which were observed to be greater than the variations for the two cases where the deviation between modes is negligible. Figures 3 and 4 show the results of the BER measurements of the TWTA at saturation, for bands B and C, respectively. In Table III(a), a comparison was made of the measured distortions between frequency bands with the TWTA at saturation. In general, distortions between frequency bands were greater for bands A and C, corresponding to the larger BER degradations observed in these bands. In particular, the amplitude variation and AM/PM conversion appear to greatly influence the BER performance. Table III(a) shows that bands A and C which have significant transmission distortions have greater variation in both measured distortion and BER performance than band B, which has relatively low distortion. The result is that system power level changes can be implemented with negligible change in BER performance when the channel transmission distortions are small. When such distortions are large, the BER performance varies significantly from mode to mode.

Further evidence of the effects of the system amplitude response on BER performance is given in Fig. 5. The amplitude response for the three bands is plotted in Fig. 5(a) (for the TWTA in the medium power mode at the 1 dB compression point). The corresponding BER curves are shown in Fig. 5(b). In most of the cases tested, it was observed that a flatter amplitude response resulted in a better BER performance.

It is significant to mention that in all cases observed, the system BER performance was best with the TWTA at saturation. The amplitude response at the the three operating points for frequency band C is shown in Fig. 6(a) (with the TWTA in the medium power mode). The corresponding BER curves are shown in Fig. 6(b). Note that for a given Eb/No, the bit-error rate further increases with the TWTA operating in 1-dB compression and in the linear region. This observation also holds true for a frequency band with better system characteristics (Band B), as shown in Table III(b).

Conclusion

The results of measurements on a Ka-band communications system simulator with variable transmitted signal power capability have been presented. This variable power capability, implemented with a multi-power-mode TWTA, can be useful in compensating for rain attenuation. It was shown that these signal power level changes can be implemented without degradation of bit error rate when other transmission distortions are small. When transmission distortions are large, significant variations in bit error rate occur between power modes.

References

1. Bagwell, J.W., "A System for the Simulation and Evaluation of Satellite Communication Networks," AIAA Paper 84-0680, Mar. 1984.

2. Kerczewski, R.J., and Shalkhauser, K.A., "Automated Testing of Developmental Satellite Communications Systems and Subsystems," NASA TM-87070, 1985.

3. Tamashiro, R.N., "20 GHz, 75 Watt Helix Traveling Wave Tube for Space Communications," NASA CR-168271, 1984.

4. Biess, J.J., Chester, M.S., and Lee, S.J., "Power Processing Unit for 75 Watt RF, 20 GHz Traveling Wave Tube," NASA CR-174727, 1984.

TABLE I. - TWTA OPERATIONAL DATA
[F = 18.5 GHz at saturation.]

TWTA mode	Beam current, mA	Anode voltage, kV	Cathode voltage, kV	Output power, W
Low	22.5	-5.2	-9.8	5.1
Medium	42.3	-2.4	-9.9	18.6
High	57.9	-.64	-10.10	34.7

TABLE II. - Eb/No DEGRADATION (dB) FROM IDEAL AT BIT ERROR RATE OF $5x10^{-7}$

Frequency band	Operating point	Low mode	Medium mode	High mode	Eb/No between modes
A	Saturation	1.23	1.35	1.99	0.76
A	1 dB Compression	1.48	1.90	2.75	1.27
A	Linear	1.69	2.04	3.41	1.72
B	Saturation	.99	.93	1.06	.13
B	1 dB Compression	1.57	1.52	1.63	.11
B	Linear	1.46	1.76	2.16	.70
C	Saturation	2.46	2.02	1.70	.76
C	1 dB Compression	3.32	3.85	3.05	.80
C	Linear	4.46	4.47	3.93	.54

TABLE III. - COMPARISON OF CW AND DIGITAL TRANSMISSION DATA

(a) Comparison for three frequency bands at saturation

Frequency band	Power mode	Amplitude variation[a]	Group delay[b]	AM/PM deg/dB	3rd Order intermod[c]	System noise[d]	Eb/No[e]
A	Low	1.40	1.74	5.29	6.6	-59.7	1.23
A	Med	2.90	2.44	5.19	8.4	-57.9	1.35
A	High	3.44	3.26	4.56	8.7	-56.6	1.99
B	Low	1.44	1.79	2.93	8.3	-62.5	.99
B	Med	1.72	2.11	1.06	5.9	-64.5	.93
B	High	1.90	2.33	2.51	7.4	-61.3	1.06
C	Low	6.74	2.55	5.39	9.1	-67.4	2.46
C	Med	3.06	2.96	5.27	10.0	-61.3	2.02
C	High	4.24	3.20	5.31	8.3	-61.5	1.70

(b) Comparison for frequency band B

Power mode	Operating point	Amplitude variation[a]	Group delay[b]	AM/PM deg/dB	3rd Order intermod[c]	System noise[d]	Eb/No[e]
Low	Sat	1.44	1.79	2.93	8.3	-62.5	.99
Low	1 dB	2.48	2.00	2.77	13.7	-67.7	1.57
Low	Lin	3.54	1.24	1.83	23.5	-67.6	1.46
Med	Sat	1.72	2.11	1.06	5.9	-64.5	.93
Med	1 dB	1.78	1.84	3.64	12.3	-65.9	1.52
Med	Lin	3.38	1.62	.61	25.4	-64.6	1.76
High	Sat	1.90	2.33	2.51	7.4	-61.3	1.06
High	1 dB	2.44	1.87	2.55	13.4	-64.6	1.63
High	Lin	3.02	2.66	1.79	28.0	-63.6	2.16

[a]Largest peak-to-peak amplitude variation over 330 MHz band (in dBm).
[b]Largest peak-to-peak group delay variation over 330 MHz band (in nanoseconds).
[c]Level of highest third order intermodulation products produced from two CW signals spaced at Fo+25 MHz and Fo-25 MHz (in dB below the fundamental CW signals).
[d]Band-limited noise power measured at the demodulator input with no signal present and no downlink noise added (in dBm).
[e]Additional Eb/No required to maintain a bit error rate of $5x10^{-7}$, as measured from the theoretical bit error rate curve (in dB).

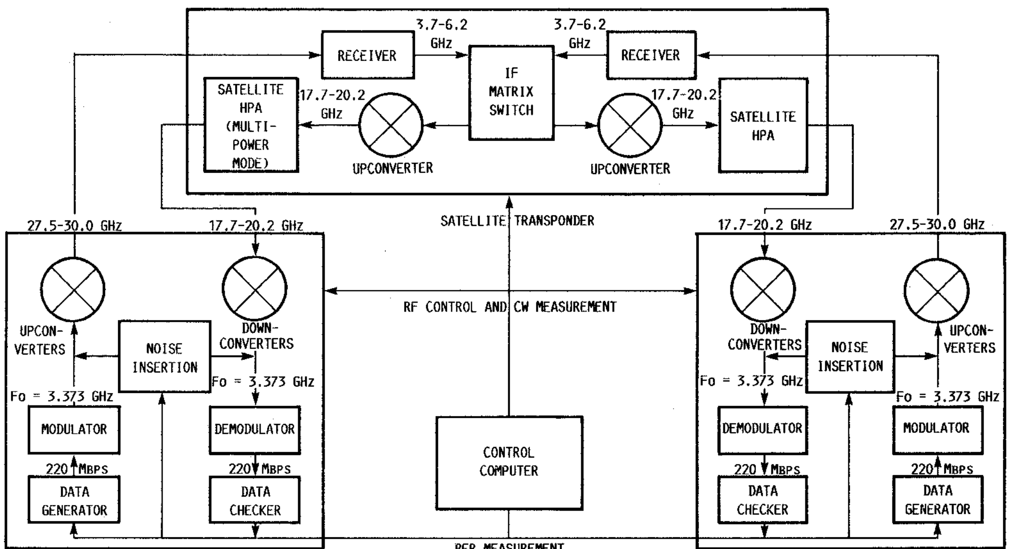

FIGURE 1. - KA-BAND SATELLITE SYSTEM SIMULATOR BLOCK DIAGRAM.

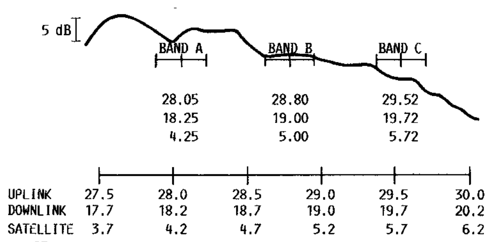

FIGURE 2. - SPECTRAL LOCATION OF TEST BANDS (APPROXIMATE LINEAR FREQUENCY RESPONSE IS SHOWN).

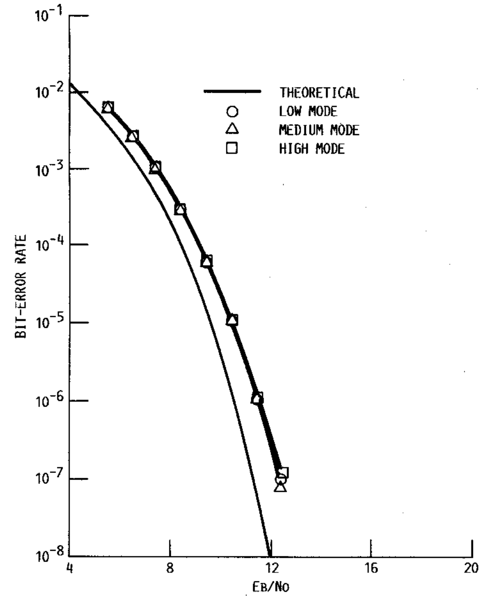

FIGURE 3. - BIT-ERROR RATE PERFORMANCE FOR BAND B AT SATURATION.

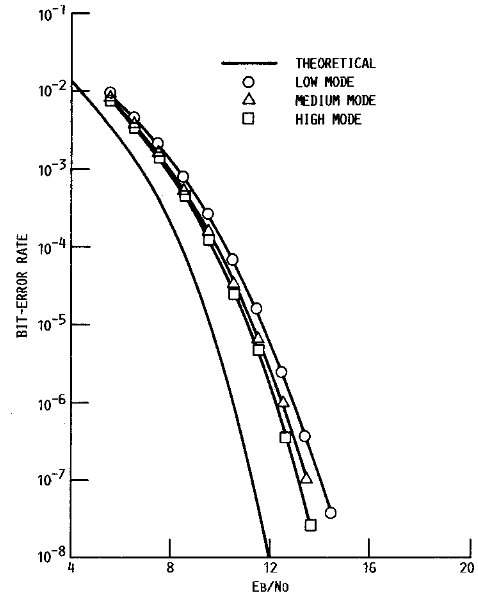

FIGURE 4. - BIT-ERROR RATE PERFORMANCE FOR BAND C AT SATURATION.

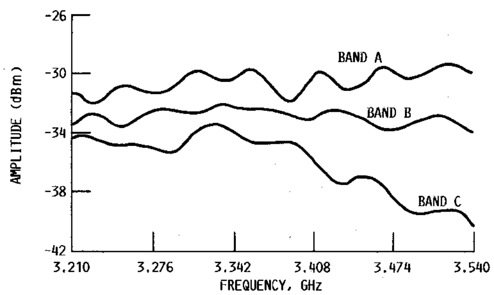

(A) FREQUENCY RESPONSE.

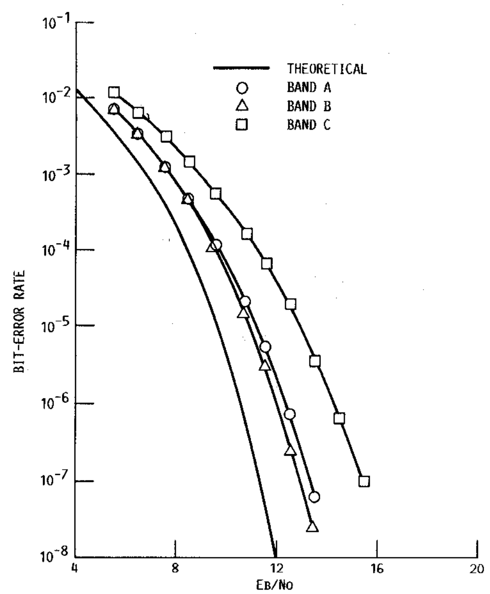

(B) BIT-ERROR RATE PERFORMANCE.

FIGURE 5. - MEDIUM POWER MODE AT 1-dB COMPRESSION.

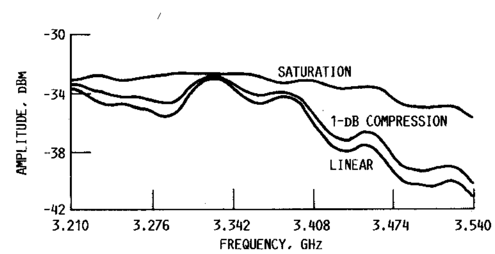

(A) FREQUENCY RESPONSE.

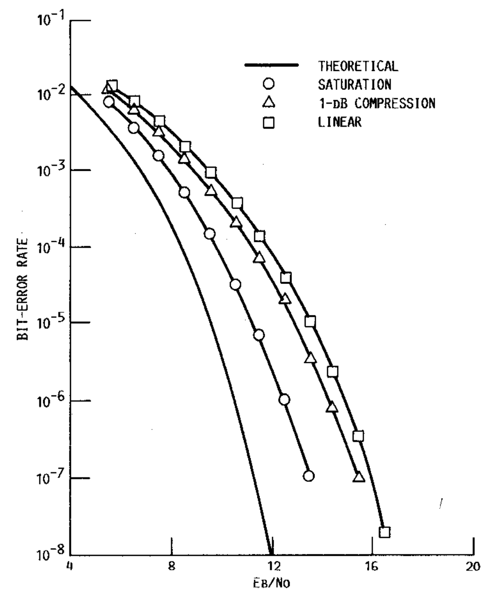

(B) BIT-ERROR RATE PERFORMANCE.

FIGURE 6. - BAND C IN MEDIUM POWER MODE.